Visible-light activated black organotitanias: How synthesis conditions influence their structure and photocatalytic activity

J. Jiménez-López,[a,b] N. Linares,[a] E. Serrano,*[a] J. García-Martínez*[a]

Abstract: A series of low temperature visible light-activated black organotitanias were synthesized through a sol-gel strategy allowing for the *in-situ* incorporation of *p*-phenylendiamine (PPD) in the framework of anatase nanoparticles. The effect of the synthesis conditions on the crystalline structure and photocatalytic activity of these materials was assessed by a number of characterization techniques, which revealed a small crystalline domain size (4.6-5.5 nm), the effective incorporation of the PPD inside the nanoparticles, and a significant reduction in the band gap of these materials (from 3.2 eV to 2.7-2.9 eV). The systematic study of the synthesis parameters allowed us also to significantly reduce the solvent used for the preparation of these black organotitanias (a 20-fold), as well as the crystallization time, without compromising the structural properties and photocatalytic activity of these materials. The organotitanias with the highest PPD content and high crystallinity result in the best performing materials in the photocatalytic degradation reaction of Rhodamine 6G under both UV and visible light irradiation.

Introduction

The quest for materials able to efficiently harvest solar light is one of the major challenges of our time. Titania (TiO_2) is one of the most widely studied solids for this task; however, its overall efficiency for solar-driven applications is limited to the UV range due to its wide band gap (3.2 eV, for the anatase phase). Currently, the main approaches to improve its sunlight-driven photocatalytic efficiency are band gap narrowing and photosensitization.[1] In the former, metal-ion implantation or non-metal doping[2-7] in the titania generates donor or acceptor states in its band gap. Usually, metal doping leads to decreased crystallinities due to the formation impurity phases while titanias prepared by non-metal doping lacks of absorption in the IR range of the solar spectrum.[8] The visible-light response of titania can also be enhanced by sensitization with suitable organic or metal-coordination dyes, quantum dots, or even plasmonic nanoparticles, able to inject electrons into the conduction band (CB) of the titania upon absorption of visible light, without modifying its electronic properties.[9-19] The main drawbacks of this method are the leaching of the dyes attached to the titania surface and the high charge carrier recombination.[10-15, 20] Another type of sensitization mechanism is based on the charge transfer between surface adsorbate and semiconductor particle, in which the electron is photoexcited directly from the ground-state adsorbate to the CB of the semiconductor.[21] In this sense, C60-based sensitized titanias[21] or the modification of TiO_2 with graphitic carbon nitride[22, 23] have received significant attention due to their visible-light photocatalytic activity and efficient charge carrier separation.

In 2011, Chen *et al.* developed an alternative approach to improve both the visible and the infrared optical absorption of titanias, which was based on the partial hydrogenation of TiO_2 (*self-doping)*.[24, 25] Because of its dark colour, this material is generally referred as 'black titania'. It consists in a TiO_2 nanocrystal core and a highly disordered surface where dopants are introduced.[24]. Since then, this promising yet costly alternative to traditional doping, has triggered world-wide research interest because of its enhanced solar absorption and its superior photocatalytic activity.[26-35] Most of the different synthetic approaches developed to prepare black titanias (in some cases called 'black anatase titanias', BAT) are based on partial reduction of (white) titania nanoparticles, namely i) an aggressive hydrogenation treatment, and ii) incomplete oxidation from low-valence-state Ti species. These two treatments are capable, in most cases, of forming defective black titania with a high concentration of Ti^{3+} species. [8, 26-37]

We have pioneered a completely different strategy for enhancing the sunlight-driven photocatalytic efficiency of titania-based materials.[38, 39] Our approach, which is not based on the partial reduction of the titania, consist in the incorporation of dyes into the anatase framework during their synthesis through the so-called "Sol-Gel Coordination Chemistry".[40] By using this technique, we have synthesized a wide range of highly efficient and stable heterogeneous catalyts based on hybrid mesoporous metal complex-metal oxide systems.[41-46] In the case of titania-based materials, this novel synthetic approach takes advantage of organic or coordination compounds (dyes) able to coordinate to the Ti(IV) atom of titanium alkoxides to form multimetal coordination compounds, which will be subsequently used as organotitania precursors. These precursors are then hydrolysed at room temperature to form a gel (containing the dyes), which is then crystallized into the anatase structure at low temperature (ca. 80 ºC). These dyes, which are highly dispersed in the bulk of the semiconductor, allow for very efficient electron injection into its CB and show outstanding stability against both degradation and leaching of the dye.[38, 39]

By using this strategy, a series of visible-light activated hybrid titanias have been produced, showing a remarkable photocatalytic activity under both UV and visible light irradiation. The incorporation of neutral (e.g. Ru(II) N3) or cationic (e.g.

[a] J. Jiménez-López, Dr. N. Linares, Dr. E. Serrano, Prof. Dr. J. Garcia-Martinez
Laboratorio de Nanotecnología Molecular, Departamento de Química Inorgánica
Universidad de Alicante
Ctra. San Vicente-Alicante s/n, E-03690 Alicante, Spain.
E-mail: elena.serrano@ua.es, j.garcia@ua.es; www.nanomol.es

[b] Current address: J. Jiménez López
Institute of Chemical Research of Catalonia (ICIQ)
Barcelona Institute of Science and technology (BIST)
Av. Països Catalans, 16, E-43007, Tarragona, Spain

Supporting information for this article is given via a link at the end of the document.

$[Ir(ppy)_2(3,3\text{-}H_2dcbpy)]PF_6$) dyes inside anatase nanoparticles by this technique yielded visible light-activated hybrid materials with an exceptional stability against leaching or photodegradation of the dyes.[39] These solids exhibit much higher photocatalytic activity, under both UV and visible light, than the related dye-sensitized titanias prepared by post-synthetic grafting of the dye over the surface of the control titania.[39] Lately, we integrated our hybrid titania containing the Ru(II) N3 dye into a photoelectrode of a low temperature dye-sensitized solar cell (lt-DSCC) obtaining the highest efficiency reported so far for titania-based lt-DSSC (8.75 %).[47] By using organic compounds, namely *p*-phenylenediamine (PPD) and dihydroxypyrimidine, hybrid organotitanias with excellent optical properties were obtained. More specifically, a black organotitania able to absorb in the whole visible range was produced by incorporating PPD in anatase nanoparticles during their synthesis. Hence, we called this material black organotitania. In this case, the black coloration is due to the partial oxidation of the PDD during the crystallization step at 80ºC, and not to the presence of a disordered phase and/or Ti^{3+} species, as these were not observed by XPS.[38] This material shows a remarkable reduction in its band gap (from 3.2 eV to 2.74 eV) and outstanding photocatalytic activity under visible light, even after several photocatalytic cycles.[38] Recently, Szaciłowski *et al*.[48] used the same approach for the incorporation of the photosensitizer 4-dihydroxyanthraquinone in titania-based nanocomposites for their applications in optoelectronic devices, proving the versatility of our methodology.

The aim of this paper is to systematically study the influence of the synthesis parameters in the crystallinity, porosity, optical properties and photocatalytic activity of a series of black organotitanias prepared by the *in-situ* incorporation of PPD during their synthesis. Our previously reported black organotitania was prepared using very large amount of water (125 ml) and ethanol (35 ml) per gram of titania and long hydrolysis and crystallization times (24 h).[38] A second goal of our study is to reduce these parameters without compromising the main structural properties and photocatalytic activity of the final materials.

Results and Discussion

The synthesis of the black organotitanias (TiO_2-PPD) was carried out following our previously described methodology.[38] First, a complex between the titania precursor, in this case, titanium tetrabutoxide (TBOT), and PPD was formed in absolute ethanol at room temperature, through the coordination of the amine groups of the PPD with the titanium atom of the TBOT. This dinuclear complex was used as organotitania precursor for the synthesis of our black organotitanias (equation 1) by its hydrolisis at room temperature. Finally, the mixture was held at 80 ºC in order to obtain the anatase structure (see the Experimental Section for details). The black colour of these organotitanias is due to the partial oxidation of the PPD, which takes place mainly during the crystallization step at 80ºC, leading to a mixture of aromatic imine species (p-phenylenequinone diamine) and PPD, which are responsible of the darkening of these organotitanias.[38]

$$2Ti(OBu)_4 + PPD \xrightarrow[RT]{EtOH_{abs}} [Ti_2(L)_2(NH_2PhNH_2)(OBu)_8],\ L = EtOH \quad (1)$$

This dinuclear complex is particularly stable, likely due to the formation of species with the following stoichiometry $[Ti_2(L)_2(NH_2PhNH_2)(OBu)_8]$ (L = EtOH) which are stabilized by Ti·····N and O·····H–N bonding interactions.[38, 49] The high stability of the complex allows for the incorporation of the PPD inside the titania framework during the synthesis, causing some local distortions in the crystalline network, as confirmed by DFT simulations (Figure 1). The model in Figure 1 represents a bulk TiO_2 anatase crystal in which one Ti and two O atoms were removed and one PPD molecule was incorporated. After annealing and relaxation, the model remains anatase-like showing the N atoms positioned above and below the C-C bonds, due to some Ti·····N and O·····H–N bonding interactions (Figure 1A), as well as the local distortion of the anatase structure in several regions caused by the PPD incorporation (Figure 1B).

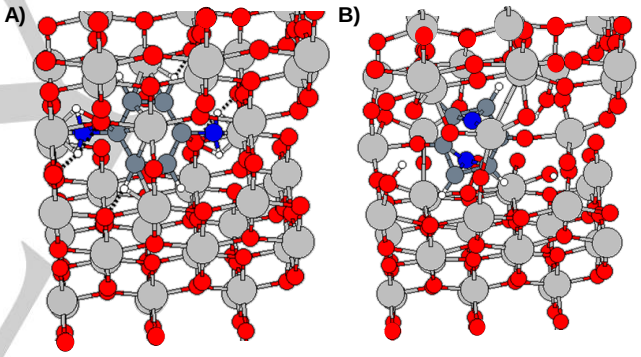

Figure 1. DFT simulations of a TiO_2-PPD black organotitania in which the PPD is incorporated inside the anatase structure. The models show **(A)** the Ti…..N and O…..H–N bonding interactions and **(B)** the local distortion of the anatase. Legend: O (light gray), N (blue), C (dark gray), Ti (red) H from $–NH_2$ group (white).

Using this methodology, a series of black organotitanias was obtained by varying the following synthesis parameters:

(i) the volume of water employed during the hydrolysis step for samples prepared with two ethanol-to-precursor molar ratios: EtOH/TBOT = 41 (35 ml EtOH per gram of titania) and EtOH/TBOT= 12 (10 ml EtOH per gram of titania). In both cases, 6 h of hydrolysis at room temperature and 24 h of crystallization at 80 ºC were used.

(ii) the crystallization time at 80 ºC (0-24 h) was studied for samples prepared with a molar ratio of the synthesis gel of 1 TiO_2:0.1 PPD:76 H_2O:12 EtOH.

Structural and textural properties. The effect of the volume of water employed during the synthesis of those samples prepared using a EtOH/TBOT molar ratio = 41 was analyzed by varying the water used from 5 to 125 ml. It shoul be noted that 125 ml of water and 35 ml of ethanol were used to prepare our previously reported black organotitania.[38] As observed in Figure 2 and Table 1, the water content has a great influence on the crystallinity and textural properties of the final materials.

Black organotitanias present, for $V_{H_2O} \geq 20$ ml, the characteristic peaks of the anatase structure at 2θ = 25.3° (101), 37.8° (004) and 48.05° (200) and an interplanar spacing of d_{101} = 0.35 nm (JCPDS card No. 21-1272). Both the intensity of those peaks and the crystalline domain size slightly increase with the volume of water, reaching the plateau at V_{H_2O} = 60 ml (V_{H_2O}/ V_{EtOH} = 1.71), see Table 1 and Figure 2B. However, in the case of the control TiO_2 only 10 ml of water were required to obtain well defined anatase peaks. The intensities of those peaks, as well as the crystalline domain sizes determined using the Scherrer equation, do not change significantly with the volume of water used during the hydrolysis step (see inset in Figure 2A and Supplementary Table S1 and Figure S1).

An additional diffraction peak of very low intensity appears in both TiO_2 and TiO_2-PPD at 2θ = 30.7º, which corresponds to the (121) peak of brookite. A simple comparison between the integrated intensities of the (121) peak of brookite and the (101) peak of anatase gives a brookite content of only ca. 4% after 24 h of crystallization at 80ºC.

Table 1. Structural and textural parameters of TiO_2-PPD black organotitanias as a function of the volume of water added during the hydrolysis step for samples prepared using a molar ratio EtOH/TBOT= 41 (35 ml EtOH per gram of titania).

V_{H2O} (ml)	V_{H2O} / V_{EtOH}	H_2O/ TBOT[a]	D_{XRD}[b] (nm)	I_{101}/I_{max}[b]	S_{BET}[c] (m^2/g)	V_t[c] (cm^3/g)	d_p[c] (nm)	PPD[d] (wt%)
5	0.14	19	n.c.	n.c.	378	0.21	2.6	4.2
10	0.29	38	*	0.3	371	0.22	2.6	4.4
20	0.57	76	4.6	0.7	304	0.28	5.1	2.0
40	1.14	152	4.6	0.8	272	0.39	7.0	1.6
60	1.71	228	5.3	0.9	252	0.43	8.0	2.0
125	3.57	467	5.1	0.9	226	0.35	8.0	3.4

[a] Water/TBOT molar ratio. [b] Crystalline domain size (D_{XRD}) and the intensity of (101) peak normalized with respect to the maximum intensity of the (101) peak of the control TiO_2, from XRD measurements. [c] BET surface area (S_{BET}), total pore volume at P/P_0 = 0.9 (V_t) and interparticle pore size (d_p) from N_2 adsorption/desorption isotherms at 77K. [d] PPD content as determined by TG. *Peaks were too small to perform any quantitative estimation. n.c.: non crystalline.

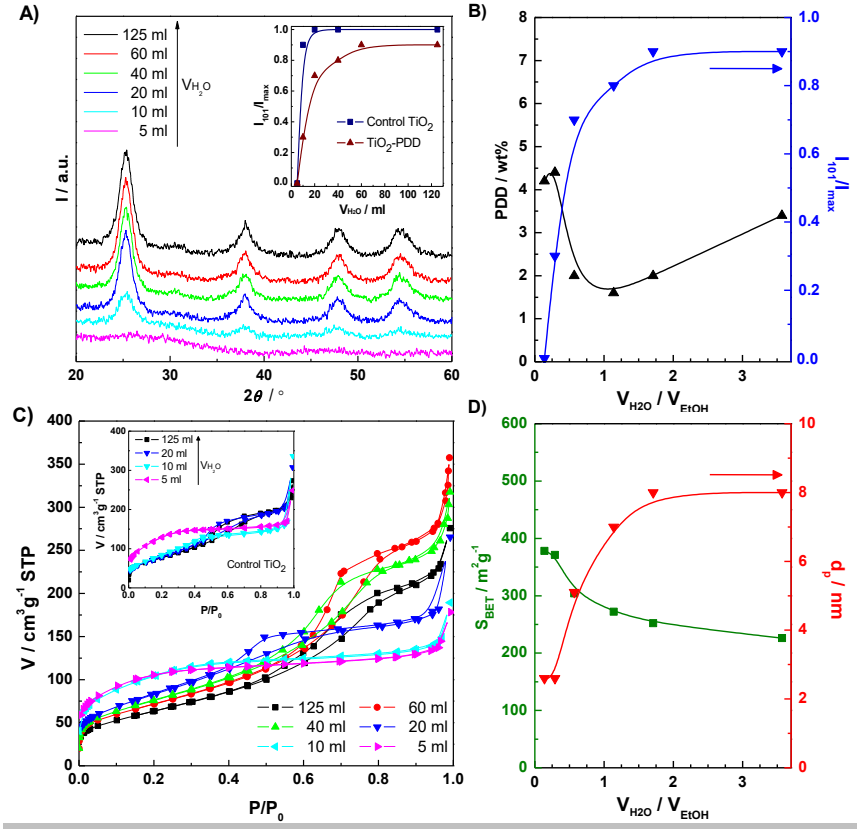

Figure 2. (**A**) XRD patterns of TiO_2-PPD black organotitanias as a function of the volume of water added during the hydrolysis step for samples prepared using a molar ratio EtOH/TBOT= 41 (35 ml EtOH per gram of titania), (**B**) the corresponding evolution of the intensity of the (101) peak normalized with respect to the maximum intensity of the (101) peak of the control TiO_2 (blue triangles) and the PPD content in the samples (black squares), (**C**) their N_2 adsorption/desorption isotherms at 77 K, and (**D**) the evolution of the corresponding textural parameters, BET surface area (green squares) and interparticle pore size (red triangles). The inset in (A) shows the intensity ratio (I_{101}/I_{max}) for both control TiO_2 (navy squares) and TiO_2-PPD (brown triangles) as a function of the volume of water used in the synthesis. Diffractograms have been vertically shifted for clarity. The inset in (B) shows the corresponding N_2 adsorption/desorption isotherms at 77 K for the control TiO_2.

Raman analyses further confirmed that the amount of brookite in these samples is negligible (see Supplementary Figure S2).[50-54] Consequently, in this work, we have assumed that the only crystalline phase is anatase to determine the crystalline domain size and the crystallinity of the samples (see Supplementary for further details). Crystalline domain sizes between 4.6 and 5.5 nm were obtained in all cases.

The textural characterization of the samples was carried out by N_2 adsorption/desorption at 77 K. For amorphous/low crystalline black organotitanias, N_2 uptake occurs at low relative pressure ($P/P_0 < 0.3$), see Figure 2C. This is characteristic of materials that present narrow mesopores (average pore diameters of 2.6 nm, see Table 1 and Supplementary Figure S3). However, crystalline black organotitanias ($V_{H_2O} \geq 20$ ml) present type IV-a isotherms with a well-developed hysteresis loop. Furthermore, for control titanias only 10 ml of water were needed to obtain this type of isotherm (inset in Figure 2B). Hence, the incorporation of the PPD requires higher volumes of water to obtain crystalline anatase nanoparticles in comparison to the control titanias. This may be due, as reported by Schubert et al.,[49] to the adduct formation from the sol-gel reaction of $Ti(OR)_4$ in the presence of ligands such as ammonia or amines, which may block the amino group and influence the hydrolysis and condensation rates of the metal alkoxide.

Besides these differences, the similar textural parameters obtained for both the control and the black organotitanias evidence that the incorporation of PPD in the anatase nanoparticles does not block the mesoporosity of these materials. Additionally, the increase of crystallinity with the addition of water during the hydrolysis step also causes a decrease in the surface area and, subsequently, an increase in the interparticle pore size that causes the mesoporosity of theses solids (Table 1 and Figure 2B,D). A similar trend was observed by Aguado-Serrano *et al.*[55] for titanias prepared using different TBOT/water molar ratios.

Furthermore, it is worth mentioning that the PPD incorporation yields are quite high (~ 70 %) when $V_{H_2O} \leq 10$ ml. Nevertheless, these yields decrease to 25-30% when intermediate volumes of water were used. For the highest V_{H_2O}/V_{EtOH} ratio, which produces a highly crystalline black organotitania, a moderate yield was obtained (53%) (Table 1).

Highly crystalline black organotitanias with small crystalline domain sizes and high porosity were obtained when using a ratio $V_{H_2O}/V_{EtOH} \geq 2$. Therefore, we decided to decrease the volume of ethanol used for the synthesis of the dinuclear complex used as organotitania precursor to a molar ratio EtOH/TBOT = 12 (10 ml of EtOH per gram of titania). In this case, different volumes of water were used during the hydrolysis step keeping the ratio $V_{H_2O}/V_{EtOH} \geq 2$ (Supplementary Table S2). Under these conditions, all the materials present anatase structure and similar crystalline domain sizes, 4.9-5.1 nm (inset in Figure 3 and Supplementary Table S2 and Figure S4). These results suggest that the crystalline structure of both the control TiO_2 and black TiO_2-PPD is not significantly affected by the EtOH/TBOT molar ratio if $V_{H_2O}/V_{EtOH} \geq 2$ (see Figure 3B). Similar conclusions can be drawn from the N_2 adsorption measurements (Figure 3 and Supplementary Figure S5). All the materials prepared under these conditions present very similar type IV-a isotherms (Supplementary Table S2). Nevertheless, the PPD incorporation yield increases as the water volume does. Incorporation yields around 50% were obtained when 60 ml of water were employed, while this percentage was halved to around 25% for V_{H_2O} = 20 and 40 ml. This observation points out that very high water-to-titania precursor molar ratio facilitates the PPD incorporation, independently of the EtOH/TBOT molar ratio. This is likely due to the dependence of the gelification rates with the amount of water, which may affect the stability of the TBOT-PPD precursor.[49] [55]

Our novel black organotitanias were also studied by TEM. As an example, Figure 4 shows some representative TEM images of a TiO_2-PPD black organotitania synthesized using 20 ml of water at two different magnifications, which evidence the polycrystalline nature of the hybrid nanoparticles. Furthermore, according to the hybrid nature of these black organotitanias, no evidences of a two-phase system or a core-shell structure during extensive TEM examination. Selected regions (shown by a red square in Figure 4A,D) of the TEM micrographs were fast Fourier transformed (FFT), Figure 4B,E. Figure 4E features various spots that can be ascribed to the anatase structure.[56, 57] The analysis of this image was useful to independently assess the interplanar spacing of the crystalline reflections and the average interplanar distance of several anatase planes. By selecting the spots shown in Figure 4E (top), the interplanar distances were calculated to be d_{101} = 0.35 nm and d_{112} = 0.21 nm.

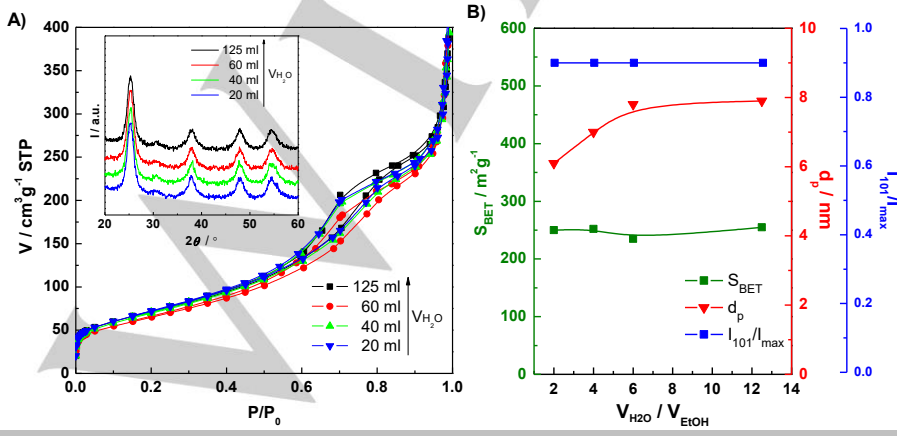

Figure 3. **(A)** N_2 adsorption/desorption isotherms at 77 K and XRD patterns (inset) of TiO_2-PPD black organotitanias as a function of the volume of water added during the hydrolysis step for samples prepared using a molar ratio EtOH/TBOT= 12 (10 ml EtOH per gram of titania). Diffractograms have been vertically shifted for clarity. (**B**) Evolution of selected textural and structural parameters as a function of the water-to-ethanol ratio used for the TiO_2-PPD synthesis.

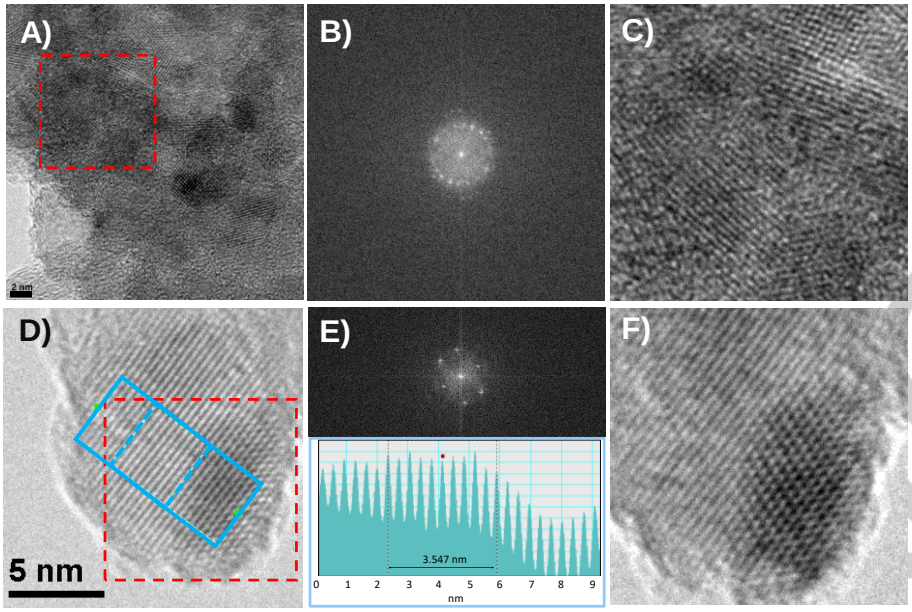

Figure 4. TEM/FFT analysis of a TiO_2-PPD black organotitania prepared using a molar ratio EtOH/TBOT= 12 (10 ml EtOH per gram of titania) and 20 ml of water per gram of titania. (**A,D**) Representative TEM micrographs at two different magnifications. Scale bars = 2 nm (A) and 5 nm (D). (**B,E**) FFT of the area marked by the red square in (A,D), respectively. (**C,F**) Image reconstruction of the area inside the red square obtained by inversing the FFT of image (B,E) showing the crystalline structure of the anatase nanoparticles. The bottom part of (E) shows the intensity line profile from the blue square in (D) used to estimate the interplanar distance.

These values are very close to those calculated from the XRD peaks: d_{101} = 0.35 nm (2θ = 25.3°) and d_{112} = 0.24 nm (2θ = 37.9°). Moreover, the intensity line profile plot shown in Figure 4E (bottom) yields an interplanar distance of 0.35 nm, which is the same value obtained from X-ray diffraction. When a larger region was analyzed, the FFT produced a partially continuous halo due to the randomly oriented nanoparticles (Figure 4B).

By comparing the results obtained for samples prepared with the two EtOH/TBOT molar ratios, it can be concluded that the solvent added during the synthesis of our black organotitanias was 20-fold reduced over our previously reported black organotitania,[38] from 125 ml of water and 35 ml of ethanol to 20 ml of water and 10 ml of ethanol, respectively, without compromising their structural properties.Only a small reduction in the PPD content was observed, which, as discussed below, does not influence the optical properties of the final materials.

With this conclusion in mind, we decided to focus on reducing the crystallization time of the black organotitanias prepared using only 20 ml of water and 10 ml of ethanol per gram of sample. Figure **5** and Table **2** show the main structural and textural parameters of the black organotitanias prepared at different crystallization times (0-24 h). After 4 h of crystallization, all the materials (TiO_2 and TiO_2-PPD) present the characteristic peaks of anatase (Figure 5). There is an increase of both the intensity of (101) peak as well as the crystalline domain size of the TiO_2 and TiO_2-PPD materials with crystallization time; although this increment is smaller in the case of black organotitanias (see Figure 5B, Supplementary Figure S6, and also column $I_{101}{}^t/I_{max}$ in Table 2 and Supplementary Table S3). Therefore, longer crystallization times were required to obtain highly crystalline TiO_2-PPD black organotitanias because of the PPD incorporation, which may delay the anatase crystallization.

In this case, the percentages of crystalline/amorphous phases were also determined using the Jensen's method[58] applied to the XRD spectra of titania/CaF_2 mixtures (50/50 wt%) (see Supplementary for details and Figure S7). As expected, the degree of crystallinity increases with time (w_{crys} in Table 2). Black organotitanias with high crystallinity (~80%) were obtained after 24 h of treatment at 80 ºC. Several authors pointed out that anatase crystallites smaller than 30 nm might produce less intense XRD peaks,[59, 60] which suggests that the values shown in Table 2 may be underestimated. This may also explain the small differences between the values obtained from the crystallinity calculated from the intensity ratio (I_{101}/I_{max}) and the percentage of crystallinity calculated using the Jensen's method (w_{crys}), columns 5 and 6 in Table 2.

To further analyze the effect on the PPD incorporation inside the anatase structure, Williamson–Hall analysis was used to quantify the lattice strain of both control and black organotitanias after 24 h of crystallization.[61] The lattice strain of the black organotitania is higher than that of the control titania (9×10^{-3} vs 6×10^{-3}, respectively) which, taking into account their similar crystallinity and crystalline domain sizes (c.a. 5 nm), is a strong evidence of the presence of PPD inside the anatase nanoparticles, causing a distortion of their crystalline lattice.

The amount of PPD incorporated remains almost constant up to 6 h of crystallization. After this time, the percentage of PPD in the samples decreases as the crystallinity of the titanias increases (see Table 2 and Figure 5B).

Regarding the textural properties of the samples, for amorphous black organotitanias (t_{crist} < 6h) N_2 adsorption takes place at P/P_0 < 0.4, which is characteristic of materials that present narrow mesoporosity (average pore diameters of ca. 2.5-3.2 nm), see Figure 5C-D and Supplementary Figure S8. At longer crystallization times, the samples present type IV-a isotherm with a well-developed hysteresis loop (inset of Figure 5C). In the case of control titanias, however, the change of the isotherm takes place only after 4 h of crystallization, and the textural properties remain almost constant for longer crystallization times (Supplementary Figure S8 and Table S3).

Table 2. Structural and textural parameters of TiO_2-PPD black organotitanias prepared at 80 ºC using different crystallization times. Molar ratio of the synthesis gel: 1 TiO_2:0.1 PPD:76 H_2O:12 EtOH.

Sample	t_{crys} [a] (h)	d_{101} [b] (nm)	D_{XRD} [b] (nm)	I_{101}/I_{max} [b]	w_{crys} [b] (%)	S_{BET} [c] (m^2/g)	V_t [c] (cm^3/g)	d_p [c] (nm)	PPD [d] (wt%)
TiO_2-PPD-0	0	n.c.	n.c.	n.c.	n.c.	430	0.34	2.5	---
TiO_2-PPD-2	2	n.c.	n.c.	n.c.	n.c.	460	0.33	2.8	5.9
TiO_2-PPD-4	4	*	*	0.2	*	375	0.39	2.8	5.9
TiO_2-PPD-6	6	0.35	4.9	0.6	55	285	0.33	3.2	4.9
TiO_2-PPD-12	12	0.35	5.1	0.7	66	245	0.33	4.7	4.8
TiO_2-PPD-14	14	0.35	5.4	0.8	66	240	0.41	4.9	3.8
TiO_2-PPD-24	24	0.35	5.4	0.9	78	240	0.50	8.0	2.6

[a] Crystallization times. [b] Lattice spacing (d_{101}), crystalline domain size (D_{XRD}), intensity of the (101) peak normalized with respect to the maximum intensity of the (101) peak of the control TiO_2, and percentage of crystallinity calculated using the Jensen's method (w_{crys}). [c] BET surface area (S_{BET}), total pore volume at P/P_0 = 0.95 (V_t) and interparticle pore size (d_p) from N_2 adsorption/desorption isotherms at 77K. [d] PPD content from the TG measurements. *Peaks were too weak to perform any quantitative estimation. n.c.: non crystalline. See Experimental Section for further details.

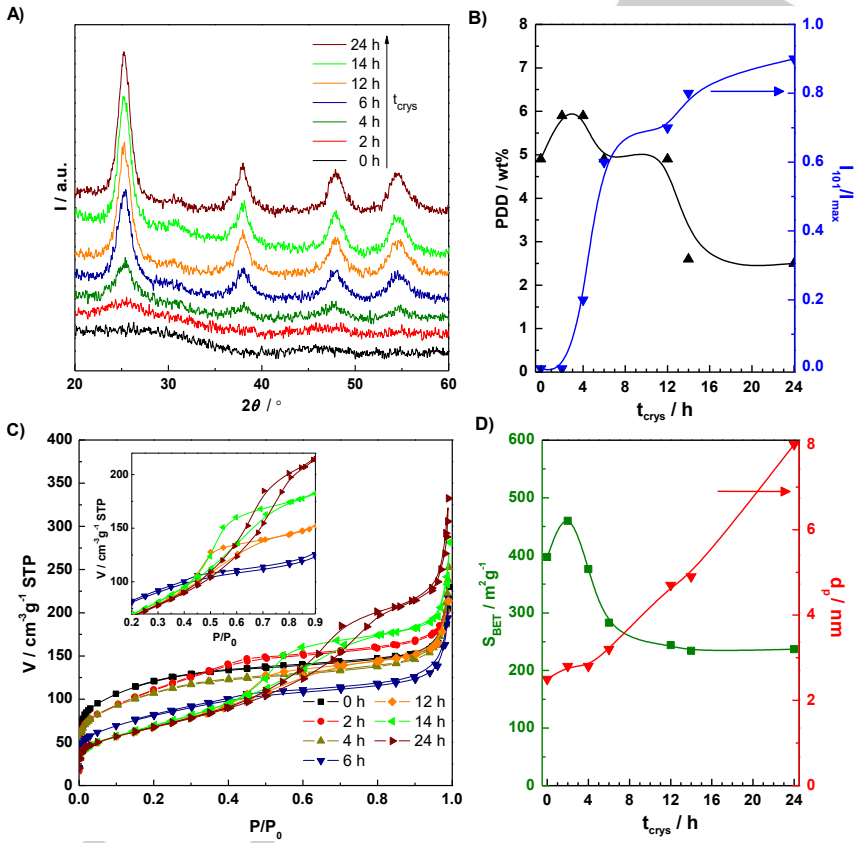

Figure 5. (**A**) XRD patterns of TiO_2-PPD black organotitanias prepared using a molar ratio of the synthesis gel: 1 TiO_2:0.1 PPD:76 H_2O:12 EtOH, as a function of the crystallization time (t_{crist}) at 80ºC. **(B)** Evolution of the crystallinity (defined as I_{101}/I_{max}) (blue triangles) and PPD content (black triangles) in these samples, **(C)** their N_2 adsorption/desorption isotherms at 77 K, and **(D)** the evolution of the corresponding textural parameters, BET surface area (green squares) and interparticle pore size (red triangles), as a function of the crystallization time.

The slower crystallization rate of TiO_2-PPD in comparison to the control titanias is likely due to the incorporation of the PPD into the anatase structure through the coordination of the PPD with the Ti atom of the TBOT, which may interfere with the formation of the anatase phase.

Scheme 1 shows the effect of both the water-to-ethanol ratio and the crystallization time on the PPD content and the main textural and structural parameters of the black organotitanias. At short crystallization times and low water/ethanol ratios (t_{crys} < 4 h, V_{H2O} / V_{EtOH} < 0.5), we observed an induction period. After 4 h, the transformation of the amorphous gels into the anatase nanoparticles occurs. At intermediates crystallization times and water/ethanol ratios part of the PPD is expelled from the structure, decreasing the PPD content.

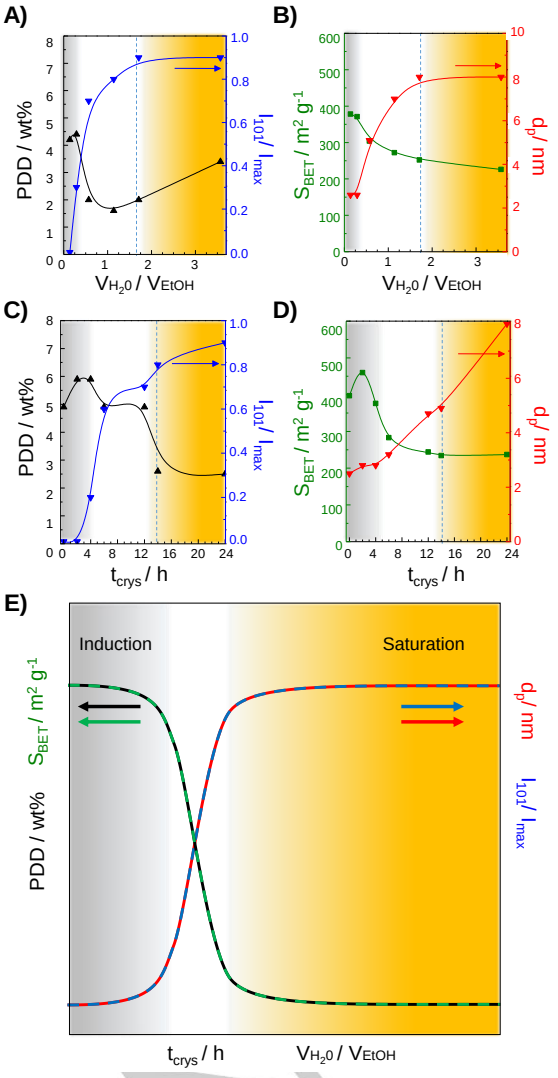

Scheme 1. Effect of both the water-to-ethanol ratio (top) and the crystallization time (middle) on the main **(A,C)** structural and **(B,D)** textural parameters of the the TiO_2-PPD black organotitanias prepared in this work. **(E)** Schematic representation of the relationship between the main structural and textural parameters of our materials as a function of the water-to-ethanol volume and the crystallization time.[7]

Moreover, the increase in the crystallinity of the samples also involves an increase in the interparticle pore size and, subsequently, a decrease in the surface area. Finally, at long crystallization times and high water/ethanol ratios (t_{crys} > 12 h and V_{H2O} / V_{EtOH} > 2) a saturation period is reached, in which all the studied parameters remain mostly constant. Hence, there is a threshold, around 12-14 h and a V_{H_2O}/V_{EtOH} = 2, which we used as an opportunity to significantly reduce the solvent used during the synthesis of these organotitanias, from 160 ml used for our previously reported black organotitania[38] to 30 ml, without compromising their structural properties and, as explained below, their photocatalytic activity. This significant solvent saving is clearly illustrated in Scheme 2.

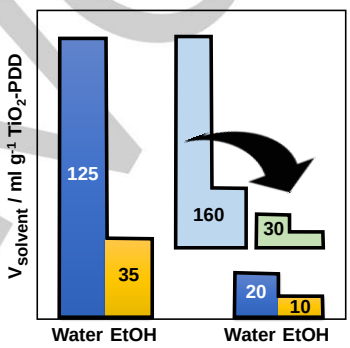

Scheme 2. Representation of the solvent reduction achieved after optimising the synthesis conditions of the black organotitanias prepared in this work (right) in comparison to our previously reported black organotitania (left).[7]

Optical properties. The optical properties of our black organotitanias were analyzed as a function of the crystallization time. The quantitative estimation of the band gap was carried out by applying the Kubelka-Munk function to Diffuse Reflectance Spectroscopy measurements (DRUV), while the maximum of the VB (VBM) was determined by XPS in the VB region (see Experimental Section for details). As shown in Figure 6A, while TiO_2 only absorbs in the UV region (λ < 400 nm, band gap 3.2 eV), TiO_2-PPD extends its absorption into the visible range, due to its black coloration.

TiO_2-PPD samples present two different absorption band edges: i) the low energy absorption band edge, around 1.4 eV, associated with partially oxidized PPD species,[38] and ii) the higher energy one, due to the indirect transitions of the anatase phase, which is remarkably red-shifted with respect to the control titania. Band gap values around 2.5 eV were obtained for amorphous/low crystalline TiO_2-PPD (t_{crist} < 12 h).[25, 62, 63] This value increased up to 2.7-2.8 eV for crystalline black organotitanias. Furthermore, the reduction in the band gap was followed by the shift of the VBM estimated by XPS in comparison to the control TiO_2 (Figure 6B,C). These results suggest a successful activation of the titania into the visible range, which evidences the modification of their electronic structure due to the incorporation of PPD.

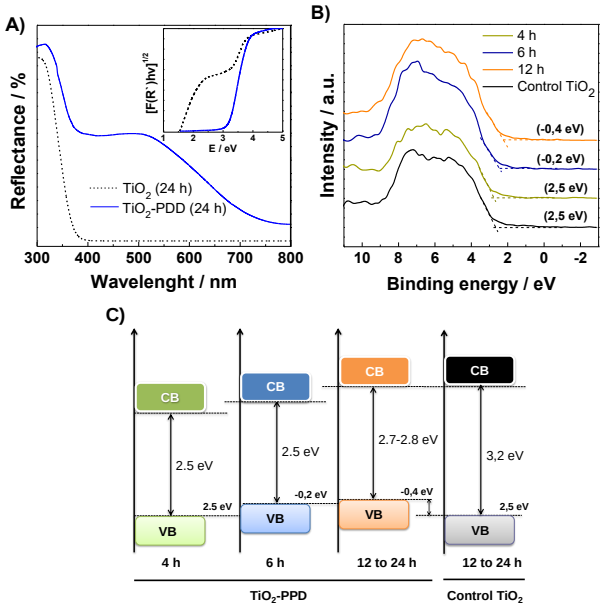

Figure 6. (**A**) DRUV spectra and Tauc plots (inset) of the black organotitania (blue line) and control titania (black dashed line) after 24 h of crystallization at 80 ºC. (**B**) XPS valence band region of black organotitanias as a function of the crystallization time for samples prepared using only 20 ml of water and 10 ml of ethanol per gram of titania (molar ratio of the synthesis gel: 1 TiO_2:0.1 PPD:76 H_2O:12 EtOH) in comparison to the control titania after 24 h of crystallization at 80 ºC. **(C)** The corresponding DOS schemes, calculated from DRUV and XPS measurements, for these solids.

Regarding the optical properties of the black organotitanias prepared using different EtOH/TBOT molar ratios, it should be noted that band gaps in the range 2.7-2.9 eV were obtained for all the crystalline black organotitanias, i.e. samples prepared using $V_{H_2O}/V_{EtOH} \geq 2$. Furthermore, the position of the VBM is slightly shifted to lower energies due to the PPD incorporation into titania framework.[38]

As expected, because the reduction of Ti^{4+} to Ti^{3+} requires very aggressive conditions, no Ti^{3+} has been detected by XPS (see Supplementary Figure S9A). Both black organotitanias and the control titania display the doublet $Ti2p_{3/2}$ and $Ti2p_{1/2}$ at similar binding energies (458.6 eV and 464.3 eV, respectively), which is consistent with Ti^{4+} in the titania lattice. Furthermore, additional lower binding energy components associated to the presence of reduced Ti^{3+}centres have not been detected by XPS after a careful deconvolution of the Ti2p peaks, which confirms the octahedral coordination of Ti^{+4} in our samples (see Supplementary Figures 9B and 9C).[38, 64, 65] Therefore, the modification of the band gap is likely caused by the incorporation of the PPD into the titania framework. As expected, the band gap of the control titanias is 3.1-3.2 eV independently of the synthesis conditions used to prepare them.

Photocatalytic activity. After studying the influence of the synthesis parameters in the structure of TiO_2-PPD black organotitanias, their photocatalytic activities were tested by following the degradation of Rhodamine 6G (R6G) in solution under both UV and visible light irradiation. Supplementary Figure S10A shows the photocatalytic activities of the series of crystalline TiO_2-PPD black organotitanias prepared using a molar ratio EtOH/TBOT= 41 (35 ml EtOH per gram of titania) as a function of the volume of water added during the hydrolysis step. Their photocatalytic activities increase as the volume of water does, as one should expected due to the increased crystallinity of these samples. The pseudophotocatalytic rate constants of the black organotitanias synthesized using 20 ml of water are similar to the one obtained with the control titania. These values increase up to 18.0 ± 2.5 min^{-1} when the volume of water used in the synthesis is 60 ml or more, which is 2.5 times higher than the control titania synthesized under the same conditions (7.2 ± 1.9 min^{-1}), see Supplementary Figure S10B. Nevertheless, black organotitanias prepared using 60 and 125 ml of water have similar surface areas, crystallinities and band gaps, which suggest that the greater amount of the dye PPD in the latter is the responsible for their higher photocatalytic activity.

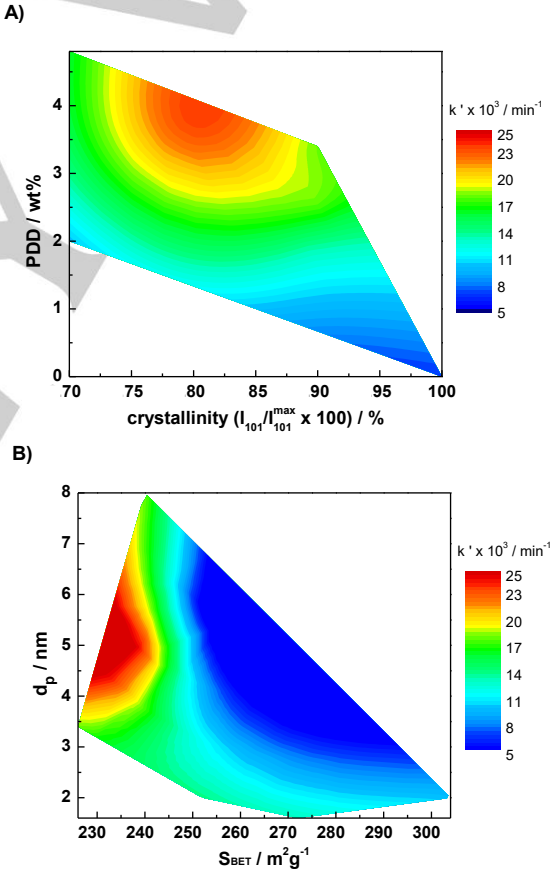

Figure 7. Photocatalytic activity of the TiO_2-PPD black organotitanias (degradation reaction of Rhodamine 6G aqueous in aqueous solutionunder UV irradiation) for samples with different water-to-ethanol volume and water-to-titania precursor molar ratios, and different crystallization times, including the control titania (0 wt% PPD). (**A**) Contour plot of the pseudophotocatalytic rate constants (k´) as a function of the PPD content and crystallinity (defined as $I_{101}{}^t/I_{101}{}^{max}$ x 100). (**B**) Contour plot of the pseudophotocatalytic rate constants (k´) as a function of the surface area and interparticle pore size.

Interestingly, when the water and ethanol volumes were reduced to 20 ml and 10 ml, respectively (Scheme 2), also a significant increase (two-three fold) in their photocatalytic activity, as compared to the control titania, was observed after 12 h of crystallization at 80ºC (Supplementary Figure S10B). The highest rate constants were obtained for those samples crystallized for 14 h, this black organotitania having the same crystallinity than the one crystallized for 24 h, but a higher PPD content.

In order to visually summarize how the structural and textural properties of the black organotitanias relate to their photocatalytic activity, Figure 7 shows the contour plots of the pseudophotocatalytic rate constants as a function of their PPD content, crystallinity, surface area and interparticle pore size. The data to make these plots are shown in Supplementary Figure S10 (each experiment was performed at least three times). The best performing materials are those with the highest PPD content and high crystallinity, with corresponds to the lowest BET areas. Furthermore, the photocatalytic activity of the black organotitania that showed the best activity under UV irradiation was also examined in the photodegradation of R6G under visible light irradiation. These results were compared with those of the commercially available P25 (see SI for details). As shown in Supplementary Figure S11, our black organotitania showed higher photocatalytic efficiency toward R6G than P25 under visible light irradiation.

Conclusions

A systematic study of the effect of the synthesis parameters on the structure, porosity, optical properties, and photocatalytic activity of a series of black organotitanias was carried out using different characterization techniques. The final goal was to identify the synthesis parameters that determine the final properties of these photoactive black organotitanias. The following conclusions can be drawn from the obtained results:

(i) The stability of the TBOT-PPD complex formed in absolute ethanol, which acts as the organotitania precursor, is affected by the water-to-ethanol and water/TBOT molar ratio, as gelification rates depends on the volume of water used. Nevertheless, the main factor influencing the PPD incorporation is the degree of crystallinity, both magnitudes being inversely dependent.

(ii) The incorporation of the PPD slows down the crystallization into the anatase structure independently on the ethanol-to-titania precursor ratio used. Similarly, the water-to-titania precursor molar ratio required for getting high crystallinity black organotitanias is higher than the one needed in the case of control titanias.

(iii) Visible light-activated black organotitanias with a remarkable reduction of its band gap (from 3.2 eV to 2.7-2.9 eV) can be obtained using different ethanol/TBOT molar ratios while keeping the water-to-ethanol volume ratio higher than 2.

(iv) The photocatalytic activity of these black organotitanias depends on both crystallinity and PPD content, being the titanias with the highest PPD content and high crystallinity the best performing materials.

In summary, visible light-activated anatase black organotitanias with excellent photocatalytic activity under UV and visible light irradiation were obtained after 12 h of crystallization at 80 ºC, with only 10 ml of ethanol and 20 ml of water per gram of titania. This means a remarkable 20-fold reduction in the solvent used with respect to our previously reported black organotitania without compromising its structural and photocatalytic activity.

Experimental Section

Chemicals. Tetrabutyl orthotitanate (TBOT, 97%), *p*-phenylendiamine (PPD, 98%), absolute ethanol and rhodamine 6G were obtained from Sigma-Aldrich and used without further purification.

Synthesis of black organotitanias. The synthesis of hybrid black organotitanias was carried out according to the procedure previously reported by us.[38] In a typical synthesis, the PPD (0.0789 g, 0.735 mmol) was first dissolved in absolute ethanol for 2 hours at 40 °C under magnetic stirring. Then, 5 g (14.7 mmol) of TBOT were added to the solution and the mixture was magnetically stirred for 40 min at room temperature. Finally, 60 g (3.3 mol) of water were added drop-wise causing the precipitation of the solid. The mixture was then kept at room temperature under vigorous magnetic stirring for 6 h, followed by treatment at 80 °C for different times (0 – 24 h) in a drying oven. The obtained solid product was washed with water and acetone, successively, filtered and dried in an oven at 100 °C for 8 hours. The molar ratio of the synthesis gel was 1 TBOT:x PPD:y H_2O:z EtOH, where x = 0 – 0.1, y = 19 – 467 and z = 3 – 41 (see Table 3 for details). **Control titanias**, i.e. organic-free titania (TiO_2 samples), were synthesized following the same procedure described above, avoiding the PPD addition.

Table 3. Synthetic conditions of TiO_2-PPD black organotitanias prepared using the different molar ratio of the synthesis gel and crystallization times assessed in this work.

No.	PPD (mol)	H_2O (mol)	EtOH (mol)	V_{H2O} / V_{EtOH}	H_2O/TBOT molar ratio	t_{crys}[e] (h)
1	0.05	19-467[a] (5-125ml)	41 (35 ml)	0.14-3.6[c]	24	24
2	0.05	76-467[b] (20-125ml)	12 (10 ml)	2.0-12.5[d]	24	24
3	0.1	76 (20 ml)	12 (10 ml)	2.0	0-24	0-24

[a] Water-to-titania precursor molar ratios: 19, 38, 76, 152, 228 and 467. [b] Water-to-titania precursor molar ratios: 76, 152, 228 and 467. [c] Water-to-ethanol volume ratios: 0.14, 0.29, 0.57, 1.14, 1.71 and 3.57. [d] Water-to-ethanol volume ratios: 2, 4, 6 and 12.5. [e] Crystallization times at 80 ºC: 0, 2, 4, 6, 12, 14 and 24 h.

Physical characterization. XRD analysis was carried out in order to study the crystalline structure of the solids. The incorporation of PPD in the organotitanias was evaluated by FTIR and XPS spectroscopy techniques, and the content of the organic compound in the final material was analysed by TG. The morphology of these organotitanias was investigated by transmission electron microscopy (TEM) using a JEM-2010 microscope (JEOL, 200 kV, 0.14 nm of resolution). Porous texture was characterized by N_2 physisorption experiments at 77 K in an AUTOSORB-6 apparatus and the results were analysed using the software package AUTOSORB1 (Quantachrome Corporation). The band

gap of both the organotitanias and the control titanias was estimated by DRUV measurements. XPS spectra of these materials were obtained in the −10 to 2 eV region to calculate the position of the maximum of their valence bands. Both techniques, i.e. DRUV and XPS in the valence band region, were combined to obtain the density of states (DOS) scheme. For comparison purposes, the same Y scale has been kept in all the graphs corresponding to each of the variables analyzed.

Photocatalytic activity of the synthesized materials was evaluated in the degradation reaction of Rhodamine 6G in aqueous solution under UV or visible irradiation.

Experimental details are described in more detail in the ESI.

Acknowledgements

Tha authors acknowledge Prof. S. Hevia and J. Mejía from the University of Chile for the DFT calculations. This work was supported by the Spanish MINECO and AEI/FEDER (ref. CTQ2015-74494-JIN). E.S. and N.L. also thank the University of Alicante (ref. UATALENTO16-03 and UATALENTO17-05, respectively). J. Jimenez acknowledges fellowship from the University of Alicante. N. Linares thanks the Generalitat Valenciana for funding (ref. GV/2016/90).

Keywords: photoactive materials • black organotitanias • visible-light activated titanias • structure • photocatalysis

[1] W. Li, Z. Wu, J. Wang, A. A. Elzatahry, D. Zhao. *Chem. Mater.* **2014**, *26*(1), 287-298.

[2] L. G. Devi, R. Kavitha. *Applied Catalysis B: Environmental* **2013**, *140-141*(Supplement C), 559-587.

[3] H. Lin, A. K. Rumaiz, M. Schulz, C. P. Huang, S. I. Shah. *Journal of Applied Physics* **2010**, *107*(12), 124305.

[4] M. Piumetti, F. S. Freyria, M. Armandi, F. Geobaldo, E. Garrone, B. Bonelli. *Catalysis Today* **2014**, *227*, 71-79.

[5] E. Wang, T. He, L. Zhao, Y. Chen, Y. Cao. *J. Mater. Chem.* **2011**, *21*(1), 144-150.

[6] W. Wei, C. Yu, Q. Zhao, X. Qian, G. Li, Y. Wan. *Applied Catalysis B: Environmental* **2014**, *146*(Supplement C), 151-161.

[7] Z. Zhang, Z. Luo, Z. Yang, S. Zhang, Y. Zhang, Y. Zhou, X. Wang, X. Fu. *RSC Adv.* **2013**, *3*(20), 7215-7218.

[8] S. G. Ullattil, P. Periyat. *J. Mater. Chem. A* **2016**, *4*(16), 5854-5858.

[9] P. A. DeSario, J. J. Pietron, D. E. DeVantier, T. H. Brintlinger, R. M. Stroud, D. R. Rolison. *Nanoscale* **2013**, *5*(17), 8073-8083.

[10] B. E. Hardin, H. J. Snaith, M. D. McGehee. *Nature Photonics* **2012**, *6*, 162.

[11] J. H. Heo, S. H. Im, J. H. Noh, T. N. Mandal, C. S. Lim, J. A. Chang, Y. H. Lee, H. j. Kim, A. Sarkar, M. Nazeeruddin, M. GrÃ¤tzel, S. I. Seok. *Nature Photonics* **2013**, *7*, 486.

[12] P. V. Kamat. *J. Phys. Chem. C* **2012**, *116*(22), 11849-11851.

[13] G. Liu, L. Wang, H. G. Yang, H. M. Cheng, G. Q. Lu. *J. Mater. Chem.* **2010**, *20*(5), 831-843.

[14] S. Mathew, A. Yella, P. Gao, R. Humphry-Baker, B. F. E. Curchod, N. Ashari-Astani, I. Tavernelli, U. Rothlisberger, M. Nazeeruddin, M. GrÃ¤tzel. *Nature Chemistry* **2014**, *6*, 242.

[15] W. Y. Teoh, J. A. Scott, R. Amal. *J. Phys. Chem. Lett.* **2012**, *3*(5), 629-639.

[16] W. Zhou, H. Fu. *ChemCatChem* **2013**, *5*(4), 885-894.

[17] P. Zhang, M. Fujitsuka, T. Majima. *Applied Catalysis B: Environmental* **2016**, *185*, 181-188.

[18] O. Elbanna, S. Kim, M. Fujitsuka, T. Majima. *Nano Energy* **2017**, *35*, 1-8.

[19] Z. Bian, T. Tachikawa, P. Zhang, M. Fujitsuka, T. Majima. *J. Am. Chem. Soc.* **2014**, *136*(1), 458-465.

[20] B. Roose, S. Pathak, U. Steiner. *Chem. Soc. Rev.* **2015**, *44*(22), 8326-8349.

[21] Y. Park, N. J. Singh, K. S. Kim, T. Tachikawa, T. Majima, W. Choi. *Chem. Eur. J.* **2009**, *15*(41), 10843-10850.

[22] X. Shi, M. Fujitsuka, Z. Lou, P. Zhang, T. Majima. *J. Mater. Chem. A* **2017**, *5*(20), 9671-9681.

[23] O. Elbanna, M. Fujitsuka, T. Majima. *ACS Appl. Mater. Interfaces* **2017**, *9*(40), 34844-34854.

[24] X. Chen, L. Liu, P. Y. Yu, S. S. Mao. *Science* **2011**, *331*(6018), 746.

[25] X. Chen, L. Liu, Z. Liu, M. A. Marcus, W. C. Wang, N. A. Oyler, M. E. Grass, B. Mao, P. A. Glans, P. Y. Yu, J. Guo, S. S. Mao. *Scientific Reports* **2013**, *3*, 1510.

[26] X. Liu, G. Zhu, X. Wang, X. Yuan, T. Lin, F. Huang. *Adv. Energy Mater.* **2016**, *6*(17), 1600452-1600n/a.

[27] M. M. Ballari, H. J. H. Brouwers. *Journal of Hazardous Materials* **2013**, *254-255*(Supplement C), 406-414.

[28] H. Cui, W. Zhao, C. Yang, H. Yin, T. Lin, Y. Shan, Y. Xie, H. Gu, F. Huang. *J. Mater. Chem. A* **2014**, *2*(23), 8612-8616.

[29] Y. H. Hu. *Angew. Chem. Int. Ed.* **2012**, *51*(50), 12410-12412.

[30] A. Lepcha, C. Maccato, A. MettenbÃ¶rger, T. Andreu, L. Mayrhofer, M. Walter, S. Olthof, T. P. Ruoko, A. Klein, M. Moseler, K. Meerholz, J. R. Morante, D. Barreca, S. Mathur. *J. Phys. Chem. C* **2015**, *119*(33), 18835-18842.

[31] Z. Wang, C. Yang, T. Lin, H. Yin, P. Chen, D. Wan, F. Xu, F. Huang, J. Lin, X. Xie, M. Jiang. *Energy Environ. Sci.* **2013**, *6*(10), 3007-3014.

[32] H. Zhang, Y. Zhao, S. Chen, B. Yu, J. Xu, H. Xu, L. Hao, Z. Liu. *J. Mater. Chem. A* **2013**, *1*(20), 6138-6144.

[33] Z. Zheng, B. Huang, J. Lu, Z. Wang, X. Qin, X. Zhang, Y. Dai, M. H. Whangbo. *Chem. Commun.* **2012**, *48*(46), 5733-5735.

[34] G. Zhu, J. Xu, W. Zhao, F. Huang. *ACS Appl. Mater. Interfaces* **2016**, *8*(46), 31716-31721.

[35] J. Kavil, S. G. Ullattil, A. Alshahrie, P. Periyat. *Solar Energy* **2017**, *158*, 792-796.

[36] W. K. Wang, M. Gao, X. Zhang, M. Fujitsuka, T. Majima, H. Q. Yu. *Applied Catalysis B: Environmental* **2017**, *205*, 165-172.

[37] X. Liu, G. Zhu, X. Wang, X. Yuan, T. Lin, F. Huang. *Adv. Energy Mater.* **2016**, *6*(17), 1600452-1600n/a.

[38] M. Rico-Santacruz, A. E. Sepulveda, E. Serrano, E. Lalinde, J. R. Berenguer, J. Garcia-Martinez. *J. Mater. Chem. C* **2014**, *2*(44), 9497-9504.

[39] M. Rico-Santacruz, Ã. n. E. SepÃºlveda, C. Ezquerro, E. Serrano, E. Lalinde, J. R. Berenguer, J. GarcÃ-a-MartÃ-nez. *Applied Catalysis B: Environmental* **2017**, *200*(Supplement C), 93-105.

[40] E. Serrano, N. Linares, J. Garcia-Martinez, J. Berenguer. *ChemCatChem* **2013**, *5*(4), 844-860.

[41] C. Ezquerro, A. E. Sepulveda, A. Grau-Atienza, E. Serrano, E. Lalinde, J. R. Berenguer, J. Garcia-Martinez. *J. Mater. Chem. C* **2017**, *5*(37), 9721-9732.
[42] A. Grau, A. Baeza, E. Serrano, J. GarcÃ-a-MartÃ-nez, C. NÃ¡jera. *ChemCatChem* **2015**, *7*(1), 87-93.
[43] N. Linares, A. E. Sepulveda, M. C. Pacheco, J. R. Berenguer, E. Lalinde, C. Najera, J. Garcia-Martinez. *New J. Chem.* **2011**, *35*(1), 225-234.
[44] N. Linares, A. E. SepÃºlveda, J. R. Berenguer, E. Lalinde, J. Garcia-Martinez. *Microporous and Mesoporous Materials* **2012**, *158*, 300-308.
[45] N. Linares, E. Serrano, A. I. Carrillo, J. Garcia-Martinez. *Materials Letters* **2013**, *95*, 93-96.
[46] M. Rico, A. E. Sepulveda, S. Ruiz, E. Serrano, J. R. Berenguer, E. Lalinde, J. Garcia-Martinez. *Chem. Commun.* **2012**, *48*(71), 8883-8885.
[47] A. Kunzmann, S. Valero, Ã. n. E. SepÃºlveda, M. Rico-Santacruz, E. Lalinde, J. R. Berenguer, J. GarcÃ-a-MartÃ-nez, D. M. Guldi, E. Serrano, R. n. D. Costa. *Adv. Energy Mater.* 1702583-1702n/a.
[48] A. Blachecki, J. Mech-Piskorz, M. Gajewska, K. Mech, K. Pilarczyk, K. SzaciÅowski. *ChemPhysChem* **2017**, *18*(13), 1798-1810.
[49] U. Schubert. *J. Mater. Chem.* **2005**, *15*(35-36), 3701-3715.
[50] C. S. Campos, E. R. Spada, F. R. de Paula, F. T. Reis, R. M. Faria, M. L. Sartorelli. *J. Raman Spectrosc.* **2012**, *43*(3), 433-438.
[51] R. M. Kadam, B. Rajeswari, A. Sengupta, S. N. Achary, R. J. Kshirsagar, V. Natarajan. *Spectrochimica Acta Part A: Molecular and Biomolecular Spectroscopy* **2015**, *137*(Supplement C), 363-370.
[52] H. Li, M. Vrinat, G. Berhault, D. Li, H. Nie, P. Afanasiev. *Materials Research Bulletin* **2013**, *48*(9), 3374-3382.
[53] W. Li, R. Liang, A. Hu, Z. Huang, Y. N. Zhou. *RSC Adv.* **2014**, *4*(70), 36959-36966.
[54] L. Zhang, Z. Xing, H. Zhang, Z. Li, X. Zhang, Y. Zhang, L. Li, W. Zhou. *ChemPlusChem* **2015**, *80*(3), 623-629.
[55] J. Aguado-Serrano, M. L. Rojas-Cervantes. *Microporous and Mesoporous Materials* **2006**, *88*(1), 205-213.
[56] P. A. Sedach, T. J. Gordon, S. Y. Sayed, T. Furstenhaupt, R. Sui, T. Baumgartner, C. P. Berlinguette. *J. Mater. Chem.* **2010**, *20*(24), 5063-5069.
[57] W. G. Yang, F. R. Wan, Q. W. Chen, J. J. Li, D. S. Xu. *J. Mater. Chem.* **2010**, *20*(14), 2870-2876.
[58] H. Jensen, K. D. Joensen, J. E. JÃ¸rgensen, J. S. Pedersen, G. SÃ¸gaard. *Journal of Nanoparticle Research* **2004**, *6*(5), 519-526.
[59] B. Ohtani, O. O. Prieto-Mahaney, D. Li, R. Abe. *Journal of Photochemistry and Photobiology A: Chemistry* **2010**, *216*(2), 179-182.
[60] B. Ohtani, Y. Ogawa, S. i. Nishimoto. *J. Phys. Chem. B* **1997**, *101*(19), 3746-3752.
[61] G. K. Williamson, W. H. Hall. *Acta Metallurgica* **1953**, *1*(1), 22-31.
[62] N. A. Deskins, J. Du, P. Rao. *Phys. Chem. Chem. Phys.* **2017**, *19*(28), 18671-18684.
[63] A. Naldoni, M. Allieta, S. Santangelo, M. Marelli, F. Fabbri, S. Cappelli, C. L. Bianchi, R. Psaro, V. Dal Santo. *J. Am. Chem. Soc.* **2012**, *134*(18), 7600-7603.
[64] L. Zhu, Q. Lu, L. Lv, Y. Wang, Y. Hu, Z. Deng, Z. Lou, Y. Hou, F. Teng. *RSC Adv.* **2017**, *7*(33), 20084-20092.
[65] B. Bharti, S. Kumar, H. N. Lee, R. Kumar. *Scientific Reports* **2016**, *6*, 32355.

Entry for the Table of Contents

FULL PAPER

Easy as hair dyes: A systematically study of the water/ethanol/titania precursor ratio allowed the development of highly visible light-activated black organotitanas with only 20 ml of water and 10 ml of ethanol per gram of sample through the *in-situ* incoporation of the *p*-phenylendiamine during their synthesis.

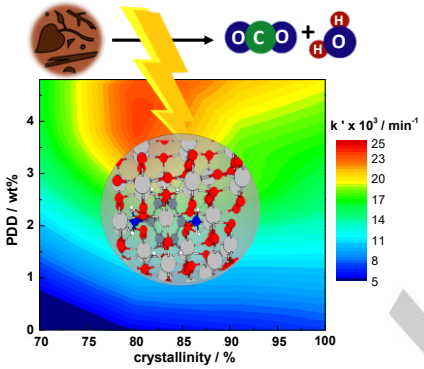

J. Jiménez-López, N. Linares, E. Serrano, J. García-Martínez**

Page No. – Page No.

Visible-light activated black organotitanias: How synthesis conditions influence their structure and photocatalytic activity